ORIGINAL ARTICLE

Drainage feasibility of a Carboniferous thin-layer limestone aquifer based on a dewatering test: Luxi coal mine, China

Jiuchuan Wei[1] · Gongyishan Yu[1] · Daolei Xie[1] · Huiyong Yin[1] · Weijie Zhang[1] · Huide Zhang[2] · Wenwu Zhou[1]

Abstract

Mine water damage is one of the main disasters threatening mine safety during production. The key to mine water hazard prevention and control is determining the main aquifer characteristics that threaten the mine and the hydraulic connections between aquifers and water diversion channels and proposing appropriate preventive measures. This paper focuses on the 16104 working face of the lower coal group in the Luxi coal mine of Shandong Province. The main water-filled aquifer that threatens the no. 16 coal mine is the Carboniferous no. 14 limestone thin-karst aquifer. Before adopting hydrophobic pressure-lowering measures, it is necessary to determine the water yield characteristics of the no. 14 limestone aquifer, the strength of recharging, and the hydraulic connection with the Ordovician limestone aquifer and to analyze and evaluate the feasibility of dredging. First, various geophysical exploration methods were utilized to comprehensively identify the anomalous water yield areas of the aquifer, which were verified by drilling methods. By combining these results with drilling and geophysical results, appropriate drainage and observation holes were selected. Second, a special water discharge stage and sequence were designed to carry out water discharge testing. By analyzing the change of water discharge and water pressure in dewatering test and the change of conventional ion concentration in water samples, the hydrogeological parameters were obtained, the hydrogeological situation was ascertained and the hydraulic connection with the Ordovician limestone aquifer was determined. The drainage time required for the aquifer to attain a safe water pressure and the amount of hydrophobicity were calculated. Through combination with the obtained hydrogeological parameters, the feasibility of depressurization was analyzed. The results show that the water yield property of the no. 14 limestone aquifer is not high, but the connectivity is good. There is a hydraulic connection between the no. 14 and the Ordovician limestone aquifers, but the connection is weak. The no. 14 limestone aquifer of the entire working surface was drained at a rate of 240 m^3/h, indicating that the aquifer has good depressurization properties.

Keywords Water discharge test · Feasibility of depressurization · Carboniferous no. 14 limestone aquifer · Water quality analysis

Introduction

Mine water disasters are major disasters affecting the safe production of mines (Guo 2016; Shi et al. 2019). A mine water disaster not only affects the normal production of a mine but may also inundate the mining area and cause numerous casualties and heavy property losses (Yang and Li 2015; Wei et al. 2017; Liu et al. 2017; Wu et al. 2018; Yin et al. 2019). China ranks first in the world in both coal production and consumption and is one of the countries most threatened by water damage (Wu 2014; Xu et al. 2015; Yin et al. 2018). Therefore, coal mine water damage prevention and control measures have become top priorities in safe coal mine production. In the past decade, coal resources in central and eastern China have gradually turned to deep mining, and the threat of mining disasters has become increasingly serious (LaMoreaux et al. 2014; Chen et al. 2016a, b; Guo et al. 2016; Qiu et al. 2016; Yang et al. 2016; Zhao et al. 2016; Yu et al. 2017; Li et al. 2018a, b, c; Shi et al. 2019).

✉ Daolei Xie
skd994469@sdust.edu.cn

1 Shandong Provincial Key Laboratory of Depositional Mineralization and Sedimentary Minerals, College of Earth Science and Engineering, Shandong University of Science and Technology, Qingdao 266590, Shandong, China

2 Luxi Coal Mine, Linyi Mining (Group) Co., Ltd., Jining 272071, Shandong, China

Among these ventures, the deep mining of the North China coalfield is generally threatened by the Carboniferous thin-layered limestone aquifer and the Ordovician karst aquifer in the coal seam floor (Sun et al. 2016; Jiang 2017). In the North China region, the Ordovician limestone has relatively high water pressure, a high water yield property, and karst development. Most thin-layered limestone aquifers and Ordovician limestone aquifers are hydraulically pressurized through fault collapse columns or fractured zones (Sun et al. 2015). Therefore, the mine production process is affected to varying degrees by the Ordovician limestone karst-confined water, and most severe water inrush accidents in coal mines are closely linked to Ordovician limestone water. The water inrush prevention and control measures in North China coalfields focus on the prevention and control of water inrushing from coal floors (Chen et al. 2016a, b; Yin et al. 2017).

In the study of the water inrush mechanism of coal seam floors, several investigators have made great progress since the 1940s after years of exploration (Motyka and Pulido-Bosch 1985; Sammarco and Eng 1986; Kuscer 1991; Mironenko and Strelsky 1993). China's research on the water inrush mechanism of coal seam floors started late, and it has made great progress since the 1960s. At present, the water inrush mechanisms of floors are primarily divided into the mechanisms of water inrushing from a floor with structural defects and from an intact floor (Li et al. 2018a, b, c). For water inrushing from floors with structural defects, Song Zhenqi, Sun Jian, Bu Wankui, Chen Zhonghui, Zhang Junfeng, Shi Longqing, etc. (Shi and Singh 2001; Zhang et al. 2009; Bu and Xu 2011; Chen et al. 2011; Song et al. 2013; Sun and Wang 2013) studied water inrushing from faults and collapse columns by means of the limit equilibrium theory and thin plate theory, combined with numerical simulations and similarity simulations. The mechanism of intact floor water inrushing mainly includes the theories of the down three zone and down four zone (Liu 1995; Li 1999; Shi and Han 2015), the theory of the key stratum (Qian et al. 1995; Xu and Qian 2004), and the theories of in situ fissures and original destruction (Wang 1992). Because the groundwater storage rule of karst water aquifers is quite different from the rule of sandstone aquifers, the water yield property of limestone is more complex than that of sandstone (Li et al. 2018a, b, c). The karst water hazards are also complex. To control the water hazards in the limestone coal seam floor, there are two main types of prevention and control technologies. One technology type is the use of grouting transformation technology for coal seam floor aquifers to rebuild the area with a high possibility of water inrushing from the coal seam floor. In this area, Zhang and Song (2013) used curtain grouting and hydrophobic pressure reduction measures to control the limestone aquifer in the Pingdingshan mining area and achieved good results. Xu et al. (2014, 2017) summarized the importance of grouting

reinforcement technologies for the floor and mining face in mitigating water inrush accidents in a large water mining area in China and introduced new developments in the technology used in theoretical analysis and engineering practice. The other technology type involves the use of drainage and pressure-decreasing technologies for coal seam floor aquifers to reduce hazardous areas (An 2018; Li et al. 2018a, b, c). Water discharge tests have also been carried out in many mines in China, but most of these tests were conducted to obtain hydrogeologic parameters (Wang et al. 2010; Pan and Wang 2011; Han et al. 2013; Zhai et al. 2014), and there was no designing of special discharge stages to analyze the feasibility of aquifer depressurization. In this paper, a special drainage feasibility test stage is designed. An innovative strategy is to judge the drainage feasibility of an aquifer by observing whether the water level in the whole area can be drained to below the safe water level, combined with determining whether the water inrush coefficient is suitable for mining requirements.

This paper selects the 16104 working face of the Luxi coal mine in Shandong Province as the research object. The no. 16 coal seam was first mined under the 16104 working face, which was mainly threatened by the thin-layered Carboniferous no. 14 limestone aquifer and the Ordovician karst aquifer. Finding out the ability of drainage and depressurization of the no. 14 limestone aquifer groundwater and whether there is a hydraulic connection between the no. 14 limestone aquifer and the Ordovician limestone aquifer is key to ensuring the safe mining of the no. 16 coal mine. Based on this, in this paper, the abnormal water yield area of the no. 14 limestone aquifer is determined using a combination of geophysical exploration and drilling, and the no. 14 limestone aquifer group hole water discharge test is designed to measure the strength of the water supply recharging in the no. 14 limestone aquifer, the relation to the hydraulic characteristics of the Ordovician karst aquifer and the feasibility of depressurization. This paper provides a reference for the prevention and control of water damage in the floor of the 16104 working face to ensure the safe mining of the no. 16 coal mine.

Study area

The Luxi coal mine is located 15.0 km north of Jining City, Shandong Province, with an area of 54.418 km². The site lies between 116°32′30″E and 116°38′00″E longitude and between 35°30′00″N and 35°37′00″N latitude (Fig. 1). The mine has adopted the vertical shaft-underground inclined shaft development mode. At present, no. 16 coal seams of Taiyuan Formation in no. 1 and no. 2 mining areas are being mined, the production level elevation is −405 m (Fig. 2). The 16104 working face is located to the west of the western
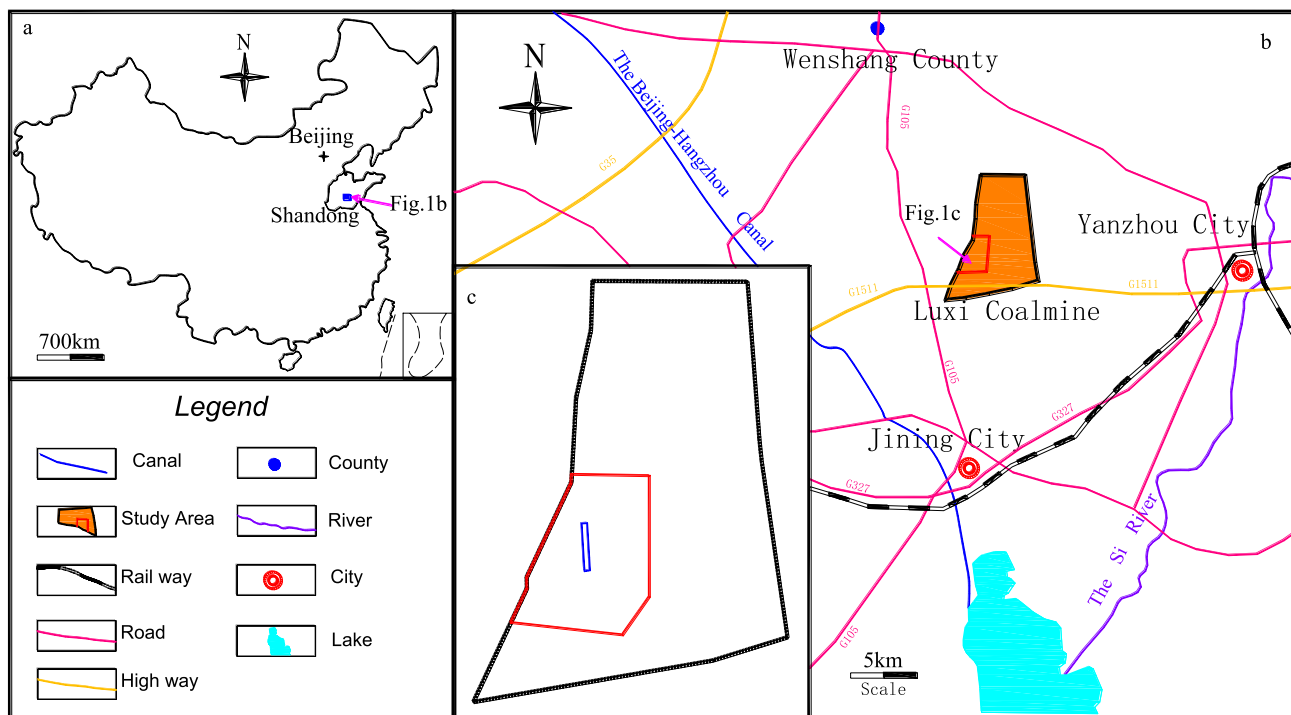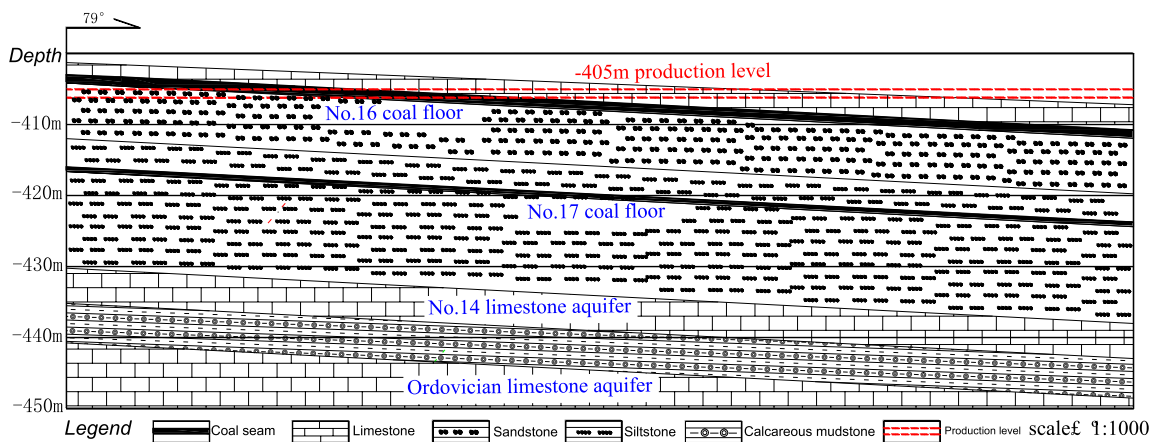
Fig. 1 Location map of the study area

Fig. 2 Stratigraphic profile of study area

no. 1 and no. 2 mining areas, adjacent to fault 3X107 in the west, south of the − 405 level tunnel wind stone gate, and adjacent to the protection pillar of the factory in the east, with a trend length of 1095 m, a tendency of 137 m and an area of 150,015 m^2.

The direct discharge aquifer of the lower coal group (mainly the no. 16 and no. 17 coals) in the Luxi coal mine is the no. 10 limestone aquifer in the no. 16 coal roof. The aquifer has weak overall water yield properties, which are only locally strong. The threat of water inrushing during

coal mining can be eliminated by releasing the water in this aquifer. The indirect water discharge aquifers affecting the no. 16 coal seam mining are the Carboniferous no. 14 limestone karst aquifer and the Ordovician limestone karst fissure aquifer.

The two aquifers are relatively close, and the total thickness is larger than 800 m. Both of the aquifers have developed karst fissures, the aquifer strength ranges from weak to strong and the head pressure is high. When the no. 16 coal seam is mined, the Ordovician limestone aquifer water may

be connected to the no. 14 limestone aquifer, and the floor may experience water bursting.

Hydrogeological exploration and water discharge tests of the no. 14 limestone aquifer were carried out at the 16104 working face. The purpose of this exploration was to determine the abnormal water yield areas, permeability, velocity difference of the runoff in each direction, influence range, hydraulic connection with the Ordovician limestone and location of the hydraulic channel connected to the Ordovician no. 14 limestone aquifer in the no. 16 coal floor, as well as to analyze the hydrogeological characteristics of the no. 14 limestone aquifer and the feasibility of depressurization under the permissible maximum capacity of depressurization; that is, whether the water inrush coefficient can be reduced under the permissible maximum drainage capacity of the mine.

Advanced exploration of the 16104 working face hydrogeology

The geophysical exploration method is the first step of water yield exploration. Several methods can be used to enhance the accuracy of detection (Ji et al. 2018). At the 16104 working face, the abnormal water yield or water-bearing structure area that is 150 m below the No. 16 coal floor is detected by transient electromagnetic exploration method to delineate the range of water content anomalies. Mine audio-frequency electrical penetration approach is used via up and down crossheading to detect the position, range and relative strength of the water yield zone in the 0–80 m interval of the coal seam under the coal seam floor in the working face, and radio-wave tunnel perspective method is used to explore the blinded structures in the working face. Combined with the location and scope of the abnormal water yield area, drilling exploration holes are scientifically arranged. A total of 55 no. 14 limestone aquifer exploratory holes and 4 Ordovician

limestone aquifer exploratory holes are arranged in 16104 working face (Fig. 3). Drilling results show that there are 20 exploration holes with water inflow between 100–200 m^3/h, 3 exploration holes for the water inflow above 200 m^3/h, and the rest are below 100 m^3/h in no. 14 limestone aquifer, and the water inflow from the exploration hole of the Ordovician limestone aquifer is relatively small, which is all below 60 m^3/h, as shown in Table 1.

By combining the locations and distribution of the abnormal areas, drilling holes are reasonably arranged; that is, the abnormal areas are delineated, and the normal water yield areas are appropriately reduced to obtain the data of the water inflow in a single hole of the whole working face. Fifty-five no. 14 limestone aquifer detection holes and four Ordovician limestone aquifer exploration holes were arranged in the 16104 working face. Among the no. 14 limestone aquifer detection holes, there are 20 holes with a specific well discharge rate between 100 and 200 m^3/h and 3 holes with a specific well discharge rate of 200 m^3/h or higher, and the discharge rates of the remaining holes are below 100 m^3/h. The specific well discharge rates of the four Ordovician limestone aquifer exploration holes are not higher than 60 m^3/h.

Design of the water discharge tests for the no. 14 limestone aquifer group holes in the 16104 working face

The purpose of the water discharge test is to ascertain the water yield property, permeability, recharge strength, location of the hydraulic connection channel and strength of the Ordovician no. 14 limestone aquifer in the no. 16 coal floor of the 16104 working face. At the same time, the hydrogeological characteristics of the no. 14 limestone aquifer and the feasibility of depressurization and pressure lowering under the permissible maximum drainage capacity of
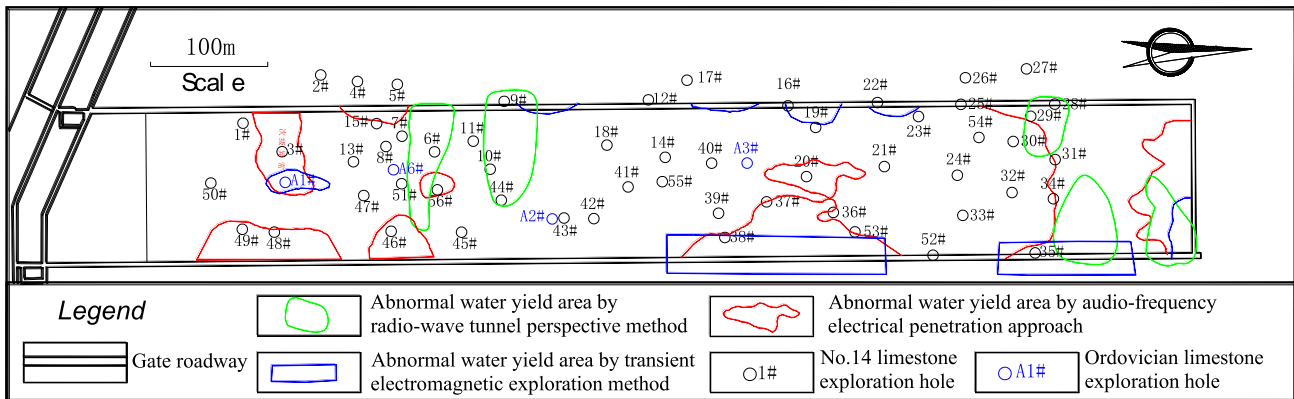

Fig. 3 Distribution map of geophysical exploration abnormal water yield area and drilling layout

Table 1 Drilling results in the abnormal water yield area of the study area

Hole number	Initial flow rate (m³/h)	Hole number	Initial flow rate (m³/h)	Hole number	Initial flow rate (m³/h)	Hole number	Initial flow rate (m³/h)
1#	15	16#	200	31#	100	46#	100
2#	3	17#	20	32#	150	47#	80
3#	5	18#	120	33#	120	48#	20
4#	15	19#	150	34#	80	49#	100
5#	13	20#	120	35#	20	50#	95
6#	120	21#	40	36#	120	51#	20
7#	110	22#	120	37#	150	52#	200
8#	100	23#	100	38#	130	53#	150
9#	80	24#	200	39#	20	54#	150
10#	50	25#	80	40#	70	55#	100
11#	100	26#	40	41#	130	A1#	20
12#	100	27#	30	42#	100	A6#	40
13#	100	28#	120	43#	65	A3#	60
14#	3	29#	30	44#	80	A2#	35
15#	50	30#	65	45#	60		

the mine are analyzed. To obtain the depressurization effect of the whole aquifer at the maximum discharge rate, prevent excessive concentration of the drainage area and avoid heterogenous dredging of the working face, the aquifer in the working face cannot be reduced to below the safe water level. In the north, south and middle parts of the working face, the drainage holes are also arranged, and no. 14 limestone aquifer holes with specific well discharge rates higher than 100 m³/h are selected as drainage holes and observation holes. All Ordovician limestone aquifer holes are also used as observation holes. Considering the results of geophysical prospecting, the data of single-hole water inflow, the locations of the boreholes, the drainage capacity of the mine and the purpose of the drainage test, 16#, 24#, 37# and 52# are selected as drainage holes and 7#, 46#, 16104-1 and 16104-2 are selected as backup drainage holes of the no. 14 limestone aquifer. The layout of the project is shown in Fig. 4.

To achieve a better drainage effect, a special drainage sequence and discharge adjustment method are designed. For this, in the first three stages, to obtain the hydrogeological parameters of the aquifer, four drainage holes (16#, 24#, 37# and 52#) are opened in the north of the working face to discharge water, and three stages of discharge occur from small to large. When the drainage in the three stages is stable, the standby drainage holes in the middle and south of the study area are opened at the maximum discharge level, and the drainage effect is analyzed to determine the feasibility of aquifer drainage.

During each stage of the discharge test, the water quantity and water level of a discharge hole are observed at all times, and the water quality is analyzed before and after the discharge test.
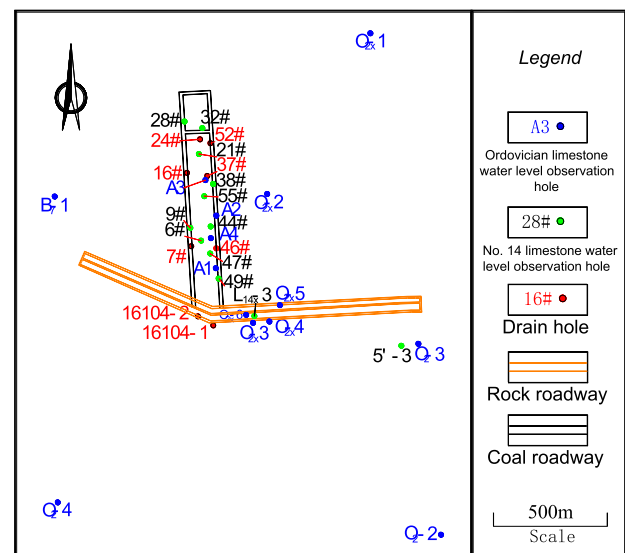
**Fig. 4** Engineering layout of the drainage test

Drainage test process and analysis

The water drainage test started at 22:00 on August 2, 2018, and ended at 17:00 on September 19. The test lasted 48 days and 19 h. The whole drainage process met the design requirements. The drainage volume of each landing is shown in Table 2.

The discharge process curves of the discharge holes were plotted according to the observation data of the discharge holes (Fig. 5). At the beginning of water discharge, 4 drainage holes (16#, 24#, 37# and 52#) were adopted. The

Table 2 List of the water flow rates

Hole number	Water flow rate (m³/h)			
	I	II	III	IV
	Start: 08.02 22:00 End: 08.14 16:30	Start: 08.14 16:30 End: 08.22 16:30	Start: 08.22 16:30 End: 09.03 10:30	Start: 09.03 10:30 End: 09.17 07:30
16#	105	29	0 (Close)	0 (Close)
24#	69	50	52	58
37#	93	61	48 (Adjust)	87
52#	73	0 (Close)	0 (Close)	0 (Close)
7#	–	–	–	74
46#	–	–	–	42
16104-1	–	–	–	25
16104-2	–	–	–	70
Total	340	140	100	356

Fig. 5 Curves of the flow rates for all holes in the drainage process
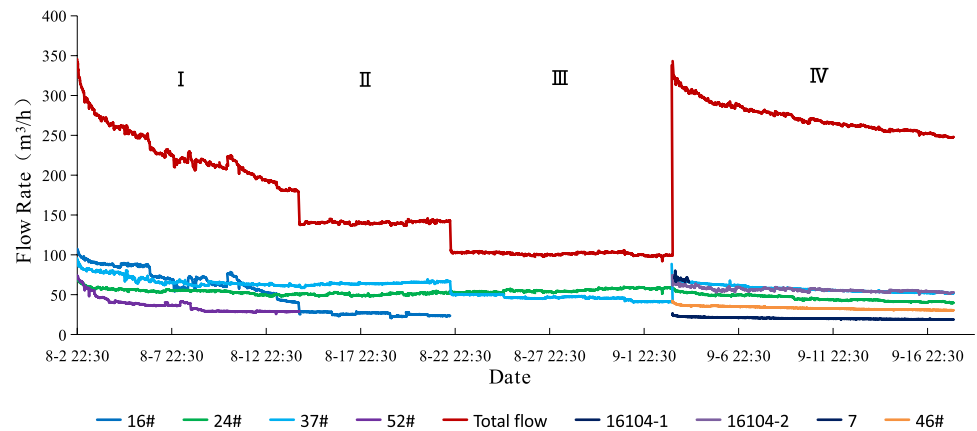
water inflow rates at single holes during drilling construction were 200 m³/h (16#), 200 m³/h (24#), 150 m³/h (37#) and 200 m³/h (52#). However, the initial flow rates of the 4 drainage holes did not reach the water inflow rates of the holes due to mutual interference after the test began, which reflects the aquifer's low water yield property. In addition, the first stage of the drainage test was in an unstable state, and as time passed, the discharge gradually decreased from a maximum to a basically stable level. The 16# flow decreased from 105 m³/h to 39 m³/h, which was a reduction of 63%; the 24# flow decreased from 69 to 50 m³/h, which was a reduction of 28%; and the flow of 37# decreased from 93 to 61 m³/h, which was a reduction of 34%. The flow rate of 52# decreased from 73 to 29 m³/h, which was a decrease of 60%. The flow rates of all 4 wells were greatly reduced, reflecting the inadequate recharging of the no. 14 limestone aquifer. The flow rates of 16# and 52# were reduced by more than 60%, while the flow rates of 24# and 37# decreased by approximately 30%. The water yield property and recharging of the No. 14 limestone aquifer are different, and the supply

directions of 16# and 52# are limited. The flow rate of each hole fluctuated greatly in the first stage, which is mainly attributable to the fact that the sediment gangue was blocked in the process of water discharge and gradually stabilized after several discharges through the discharge hole. In the second and third stages, the flow rate of each hole was basically in a stable state.

The purpose of the fourth stage was to analyze and study the feasibility of drainage of the no. 14 limestone aquifer. Because local drainage cannot drain the whole working face and based on the maximum discharge rates of 24# and 37# in the north, 7# and 46# in the middle and 16104-1 and 16104-2 in the south were opened at the same time to facilitate the drainage of the whole area of the 16104 working face. The first and fourth stages were conducted at the maximum-capacity drainage level. The total drainage rate in the middle stage of the first stage was approximately 210 m³/h, and that in the later stage was approximately 180 m³/h. The total drainage rate in the fourth stage was approximately 240 m³/h. The maximum sustainable drainage rate in the

face was 240 m³/h, and this discharge design can be used to control the aquifer during the mining period of the working face.

Analysis of the water levels of the no. 14 and Ordovician limestone aquifers

The water level data of each observation hole were recorded in the process of the water drainage test, and the duration curve of the No. 14 limestone water level (Fig. 6) and the duration curve of the Ordovician limestone water level (Fig. 7) were plotted. As shown in Fig. 6, the water level changes show typical characteristics, and the curves of each stage consist of three parts, namely, the Instantaneous change stage, the rapid transition stage, and the long stable stage.

The Instantaneous change stage

From the observation hole water level change curve, it can be concluded that the first and fourth stages of the water level followed instantaneous decline curves, and the second and third stages had instantaneous rise stages. The second and third landing stages were intermediate test stages, and the variation in the discharge flow rate was small. The flow differences between the first and second stages and between the second and the third stages are basically 40 m³/h. Therefore, the recovery and transition in the second and third stages are not apparent.

The instantaneous drop or rise in the water level reflects the overall good connectivity of the no. 14 limestone aquifer. Among the holes, 21# and 38# are the closest to the discharge center, so the drop was the largest. The distances from 28#, 32# and 55# to the water discharge center are 234, 180 and 200 m, respectively. Thus, the distances were compressed, and the water level dropped by approximately the same amount. The water level basically dropped outward in concentric circles from the water discharge center in different directions. From the above evidence, it can be inferred that the anisotropic permeability difference of the no. 14 limestone aquifer under the 16104 working face is slight. The water levels of 16104-1, 16104-2 and L14x-3, which are far from the center, decreased by 2.2, 2.61 and 1.7 m, respectively, after 10 min of the water test, and water level decline responses were observed in the three observation holes within 1 min; hence, it can be inferred that the permeability or connectivity of the no. 14 limestone aquifer is good.

The rapid transition section

In the first and fourth stages of the water level curve of an observation hole, there is a fast transitional curve, with the largest curvature occurring after the instantaneous descent section. The main reason behind this result is that the water level of the observation hole was rapidly recharged by the nearby water volume after the instantaneous descent, which further reflects the good connectivity of the no. 14 limestone aquifer in the 16104 working face.

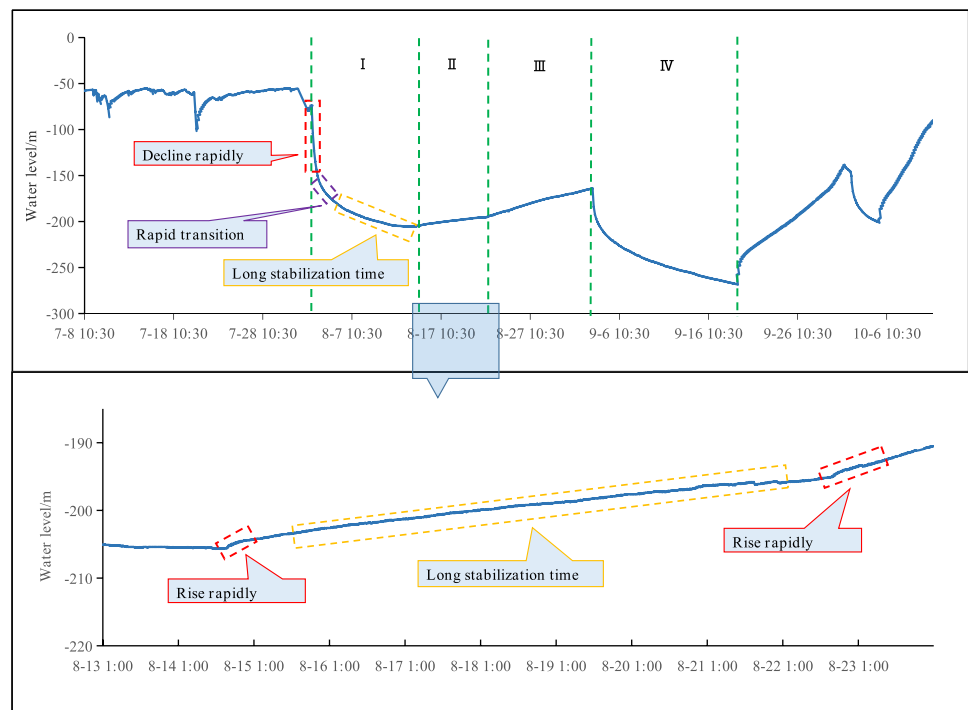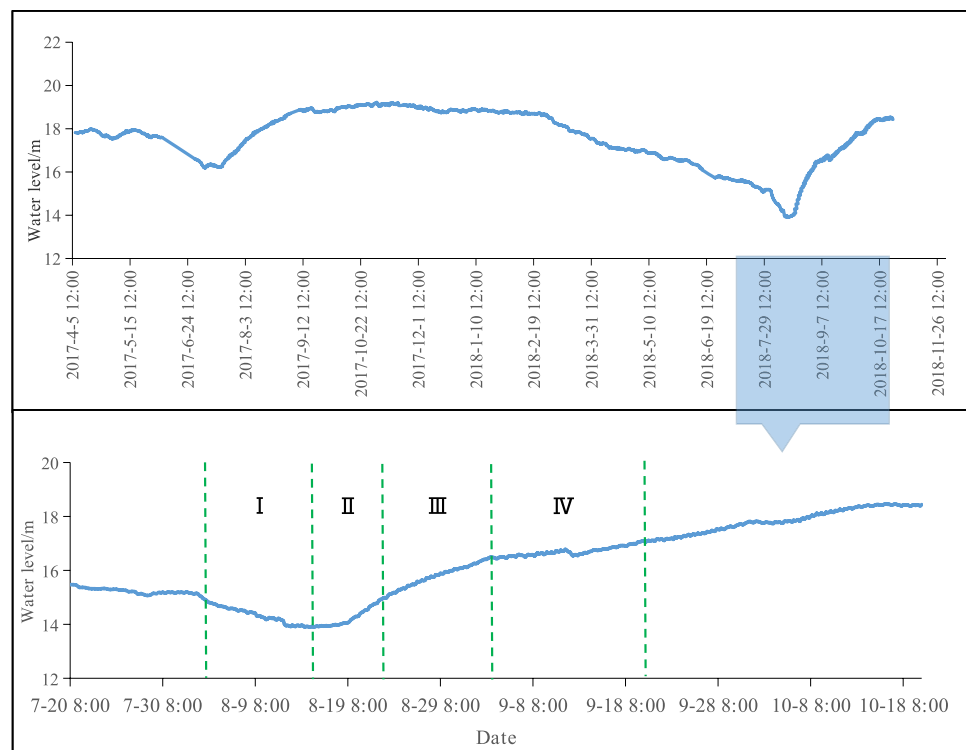**Fig. 6** The water level duration curve of the L14$_x$-3 hole

Fig. 7 The water level duration curve of the B$_7$-1 hole

The long stable stage

When nearly all of the water has been consumed, there is not enough water to replenish the continuous decline in the observation holes, which depends only on the remote water supply. If the water yield property of the no. 14 limestone aquifer is large, the aquifer can rapidly be replenished to reach stability. Although the water levels of the observation holes were nearly stable in the first half of the month, the water level had not yet reached complete stability, and most of the holes were still declining at 2.5 m/day. The decline in the water level indicates that the recharge condition of the no. 14 limestone aquifer is poor.

From Fig. 7, the water level of the Ordovician limestone decreased slowly in the first half of the year of the drainage test. Based on the data and records of the water level of the Ordovician limestone in previous years, the water level in the Luxi coal mine changed seasonally. The water level declined slowly before the end of July and the beginning of August, and then the water level rose slowly. The discharge time occurred in the turnaround period of the water level changing from falling to rising.

During the first stage, the decline rate of the water level of the Ordovician limestone was accelerated, and the time at which the water level began to rise was delayed by nearly 20 days compared with that in the preceding years. At the same time, the water level increase rate was slightly higher than that in previous years. After the drainage test, the recovery rate returned to normal. It can be seen that the discharge

of the no. 14 limestone aquifer has a precise impact on the water level of the Ordovician aquifer, but the water level of the Ordovician aquifer dropped approximately 1–2 m during the whole discharge process. Generally, the hydraulic connection between the Ordovician and no. 14 limestone aquifers is weak.

The water level of the A2 observation hole in the Ordovician aquifer is abnormal and has a strong hydraulic connection with the no. 14 limestone. The water level duration curve of the A2 hole (Fig. 8) shows that the A2 hole is very sensitive to the water discharge of the no. 14 limestone. The water level variation curve is basically consistent with the curves of the no. 14 limestone observation holes. The maximum drawdown depth of the water level in the first stage was 7.9 m, and the maximum drawdown depth of the water discharge in the fourth stage was 2.4 m. There is a notable difference between the A2 hole and other Ordovician limestone observation hole water level data. There are two possible causes of this phenomenon.

First, the hydraulic connection between the A2 hole and no. 14 limestone is attributed to cracking or poor grouting behind the well. There is a step change in the curve of the first stage of water discharge. At the beginning of water discharge, the hydraulic connection between the A2 hole and no. 14 limestone was relatively weak. After 2 days of water discharge, the hydraulic connection became stronger due to water flow erosion or an increase in pipe cracks. The decrease rate increased suddenly, which is essentially consistent with the change in the of no. 14 limestone. The reason

Fig. 8 The water level duration curve of the A2 hole
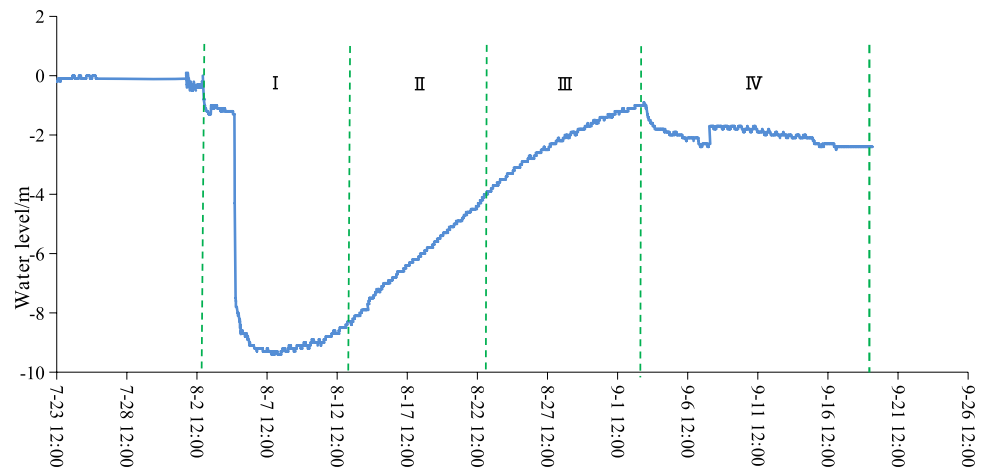
for this conjecture is that there was a case of water inrushing caused by casing breakage in the no. 28 and no. 50 boreholes after the dewatering test. In addition, the A2, no. 28 and no. 50 boreholes were drilled by the same construction team, so it is inferred that there is the possibility of breakage in hole A2.

Second, there are hidden connection channels between the no. 14 and the Ordovician limestone aquifers near the A2 hole. At present, according to the exposed situation of the working face, there are no very large faults near the A2 hole, and the possibility of a collapse column is very small; therefore, further channel exploration is needed.

It can be concluded that there must be a channel connecting the Ordovician limestone and the no. 14 limestone near the A2 hole. According to the characteristics of the water level change of Ordovician limestone during the dewatering test and the situation of the casing breakage and water inrushing during the same period, the first cause is the most likely.

Water quality analysis

To analyze the hydraulic relationship between the no. 14 and Ordovician limestone aquifers during the dewatering test, the groundwater of no. 14 and Ordovician limestone aquifers were sampled and tested before and at various stages of the test. In strict accordance with the sampling process, a total of 37 water samples were taken with 2.5 L plastic barrel, including 6 Ordovician limestone aquifer water samples and 31 no. 14 limestone water samples, which were sent to Shandong Lunan Geological Engineering Survey Institute for water quality analysis. The content of each conventional ion in the water quality sample is shown in Table 3. The sample numbers A1, A2, A3, and A6 are Ordovician limestone water samples and the other are all no. 14 limestone water samples. According to the water quality before the water drainage test and by comparing the ion contents of the

no. 14 and Ordovician limestone aquifer waters, the following conclusions were drawn.

The water quality of the Ordovician aquifer is associated with the $HCO_3^-·SO_4^{2-}·Ca^{2+}·Mg^{2+}$ contents. The TDS from 459.82 to 643.93 mg/L, with an average of approximately 571.43 mg/L. Ca^{2+} is the main cation, accounting for 27.59 to 50.69% of the cations, with an average of 44.93%, and is followed by Mg^{2+}, accounting for 26.74–38.98% of the cations, with an average of 30.51%, and Na^+, which accounts for 18.12–24.52% of the cations, with an average of 22.97%. $HCO3^-$ is the major anion, accounting for 42.98–57.38% of the anions, with an average of 51.51%. $SO4^{2-}$ accounts for 31.26–37.81% of the anions, with an average of 34.6%. Cl^- accounts for 10.78–18.63% of the anions, with an average of 13.36%. The water quality data of the Ordovician limestone aquifer show typical characteristics of limestone water, and the mineralization degree of the Ordovician limestone aquifer is comparatively low.

The water quality of the no. 14 limestone aquifer is related with the $HCO_3^-·SO_4^{2-}·Ca^{2+}·Mg^{2+}$ values. The TDS from 716.81 to 788.87 mg/L, with an average of approximately 742.08 mg/L. Ca^{2+} is the main cation, accounting for 45.27–52.01% of the cations, with an average of 50.02%. Mg^{2+} is another cation, accounting for 24.63–27.28% of the cations, with an average of 26.12%. Na^+ accounts for 19.5–28.86% of the cations, with an average of 22.71%. $SO4^{2-}$ is the main anion, accounting for 40.75–54.78% of the anions, with an average of 45.50%, followed by $HCO3^-$, which accounts for 32.21–46.27% of the anions, with an average of 41.24%. Cl^- accounts for 12.16–12.97% of the anions, with an average of 12.65%. It can be seen from the test results of the water quality samples of the no. 14 and Ordovician limestone aquifer groundwater before the dewatering test that the two aquifers groundwater in the study area have the same water chemistry type, the conventional ion concentrations in each water chemistry are similar, and the water chemistry characteristics are also the same.

Table 3 Conventional ion content of water samples

Sample number	Sampling date	Water chemistry conventional ion concentration (mg/L)							
		TDS	K^+	Na^+	Ca^{2+}	Mg^{2+}	Cl^-	SO_4^{2-}	HCO_3^-
16104-2	2017.10.31	742.08	4.81	62.24	131.42	41.23	57.05	262.32	335.33
A3#5.9	2018.5.9	572.51	4.48	51.97	96.91	35.69	40.37	156.78	342.46
A2#5.18	2018.5.18	544.27	6.58	54.25	78.89	38.31	51.92	166.46	281.82
S24#8.1	2018.8.1	727.96	4.94	62.64	130.08	40.02	56.69	258.9	321.06
S37#8.1	2018.8.1	716.81	4.62	58.47	126.95	40.84	54.6	242.37	349.59
S52#8.1	2018.8.1	734.69	4.91	67.3	127.82	39.29	53.68	262.99	328.19
S16#8.1	2018.8.1	788.87	4.76	60.56	140.81	44.78	63.23	285.01	342.46
A6#8.1	2018.8.1	643.93	4.15	47.57	115.97	41.93	53.38	202.43	328.19
A1#8.1	2018.8.1	628.71	5.18	50.63	112.58	37.9	49.93	185.01	349.59
A2#8.1	2018.8.1	459.82	7.97	57.86	45.2	38.72	53.9	147.91	214.04
A3#8.1	2018.8.1	579.39	4.64	50.98	99.15	35.62	40.32	154.21	356.73
S24#8.4	2018.8.4	691.52	4.56	69.56	113.2	38.99	51.9	253.94	292.52
S52#8.4	2018.8.4	737.94	4.78	76.61	124.27	38.77	51.94	268.14	321.06
S37#8.4	2018.8.4	784.77	5.18	78.65	125.39	43.47	58.33	317.05	285.38
S16#8.4	2018.8.4	850.72	5.07	65.62	138.68	51.97	61.81	378.44	271.11
A3#8.4	2018.8.4	565.63	4.31	52.96	94.66	35.75	40.41	159.35	328.19
S16#8.7	2018.8.7	785.22	4.28	62.47	136.62	43.19	63.25	287.17	345.31
S52#8.7	2018.8.7	787.3	4.87	82.18	122.23	38.93	55.33	301.44	336.75
S24#8.7	2018.8.7	696.87	4.13	68.64	114.11	35.88	50.58	242.25	333.9
S37#8.7	2018.8.7	814.24	5.05	81.2	124.15	41.2	59.1	328.56	322.48
S52#8.12	2018.8.12	817.44	5.06	86.03	129.98	40.66	57.19	315.53	336.75
S37#8.12	2018.8.12	833.16	5.21	81.92	134.25	42.91	59.83	325.03	339.61
S24#8.12	2018.8.12	711.09	4.22	71.7	115.09	36.98	52.33	247.49	336.75
S16#8.12	2018.8.12	792.5	4.31	62.44	138.95	44.48	64.13	290.69	342.46
S52#8.17	2018.8.17	799.95	5.31	85.01	130.81	44.03	58.71	293.77	335.32
S37#8.17	2018.8.17	827.86	5.49	82.84	138.04	45.32	59.38	318.75	328.19
S24#8.17	2018.8.17	733.3	4.56	74.91	125.17	39.27	53.34	259.42	325.34
S16#8.17	2018.8.17	803.97	4.73	68.49	143.04	47.67	64.13	295.8	328.19
S37#8.22	2018.8.22	792.82	4.9	72.93	123.78	41.91	62.21	322.79	299.65
S24#8.22	2018.8.22	724.13	4.26	66.43	116.44	38.01	58.12	268.85	311.07
BJ35#9.10	2018.9.10	488.24	2.07	179.12	7.62	4.31	30.37	72.61	353.87
S7#9.19	2018.9.19	824.6	4.46	66.29	134.63	43.36	67.56	343.45	299.65
S37#9.19	2018.9.19	753.93	3.92	59.39	125.9	40.75	65.02	296.63	293.94
S46#9.19	2018.9.19	922.76	5.61	86.69	144.19	44.68	68.49	416.96	285.38
S24#9.19	2018.9.19	719.51	4.06	68.28	114.02	35.84	58.16	275.65	299.65
S1#9.19	2018.9.19	865.59	5.06	73.85	139.32	42.7	66.64	380.77	285.38
S2#9.19	2018.9.19	884.6	5	66.75	146.12	45.19	74.92	378.19	292.52

According to the water quality sample data of the no. 14 limestone aquifer discharge holes, the water chemistry type in the working face did not change and the concentration change of various anions and cations did not exceed 10% during the dewatering test. The water quality of the no. 14 limestone aquifer did not change significantly during the test, as showed in Fig. 9. It shows that the water quality of the no. 14 limestone aquifer in the study area has not changed significantly at all stages of the dewatering test.

A piper diagram of all water samples (Fig. 10) was drawn according to the water quality test results. It can be seen from the figure that the positions of the no. 14 limestone aquifer water samples in the rhomboid region were almost unchanged in all stages of the water discharge test, indicating that the no. 14 limestone aquifer water experienced no notable mixing with water of another quality throughout the whole water test stage. Moreover, most of the 37 water samples were concentrated in the same rhomboid region, indicating that the groundwater of Ordovician and no. 14 limestone aquifer had no significant difference before and after the test. In addition, during the dewatering test, the concentrations of the conventional ions in the no. 14
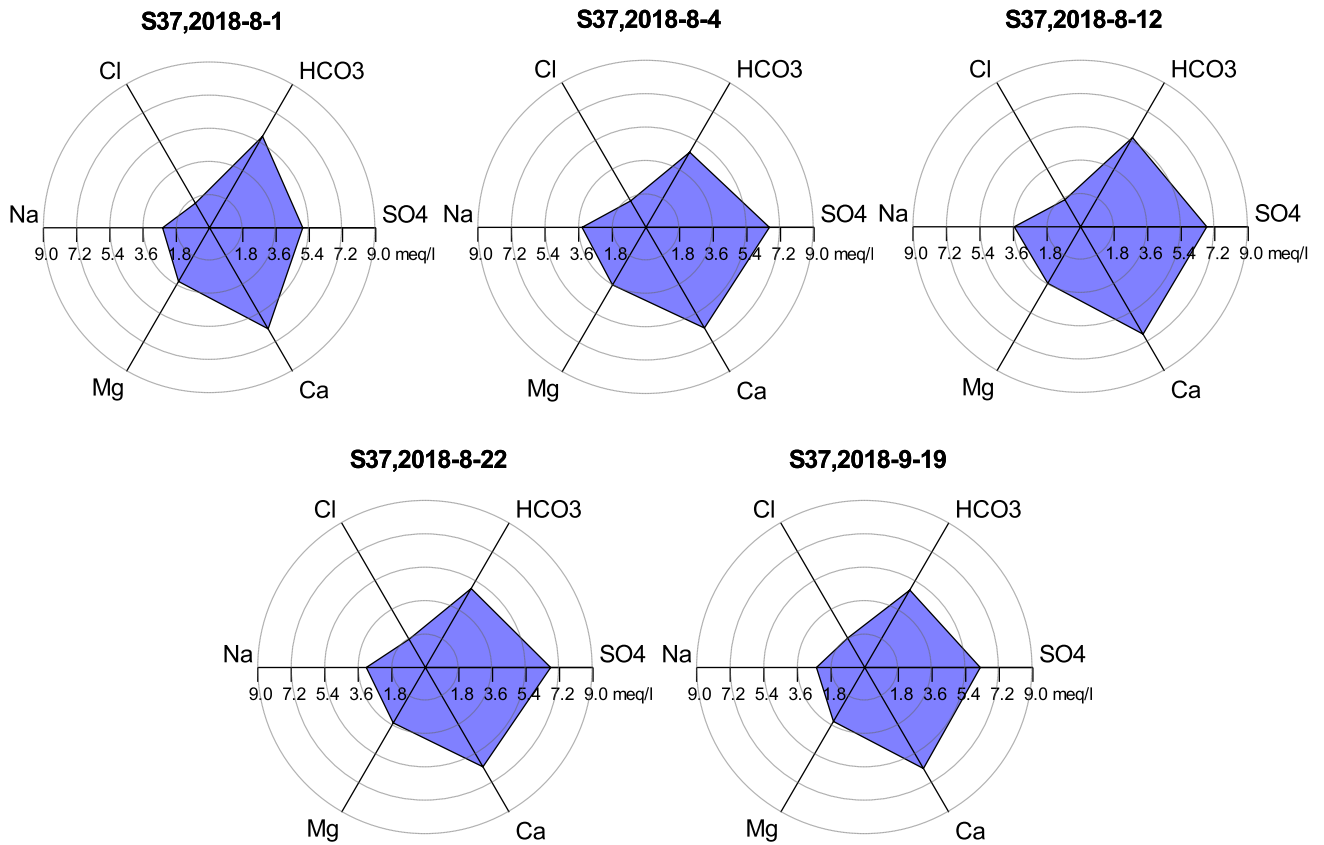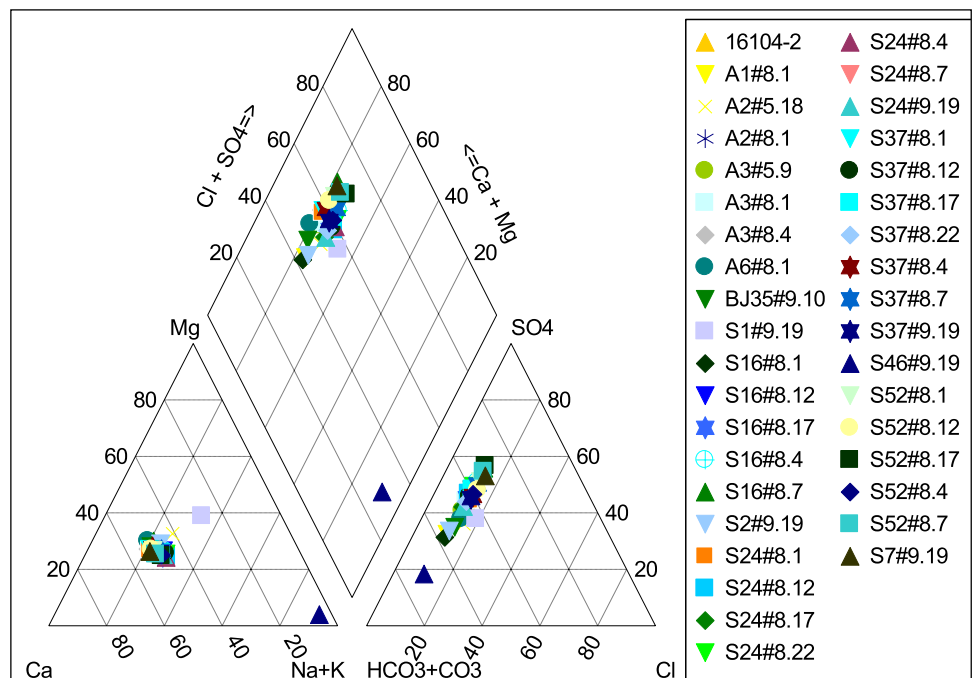
Fig. 9 Rose diagram of the water quality of the no. 14 limestone aquifer before the drainage test

Fig. 10 Water chemistry piper diagram

limestone aquifer groundwater did not change significantly. Therefore, in this area, for Ordovician and no. 14 limestone aquifer groundwater which belong to limestone water, the conventional hydrochemical analysis cannot be used to distinguish and distinguish the hydraulic relationship between them.

Feasibility analysis of depressurizing the no. 14 limestone aquifer

The first three stages of the drainage test were mainly concentrated in the northern area of the working face. The feasibility of depressurizing the no. 14 limestone aquifer in the 16104 working face was analyzed, and the effects of local and regional water drainage on the dredging effect were compared. In the fourth stage of the drainage test, 24# and 37# in the north were opened at the maximum flow rate, while 7# and 46# in the middle and 16104-1 and 16104-2 in the south were opened. The total flow rate was stable at 240 m³/h, so that the whole area of the 16104 working face could be drained. By combining these results with those of the dewatering test, the risk of water inrush and the feasibility analysis of depressurizing the no. 14 limestone aquifer were evaluated using the theory of the water inrush coefficient.

The concept of the water inrush coefficient is put forward on the basis of the study of floor water inrushing in the 1960s and through the comprehensive analysis and research of the experience of floor water inrushing in coal mines in China. It is used as the standard for water inrush prediction. In 2018, the "detailed rules for prevention and control of water disasters in coal mines" issued by the State Coal Mine Safety Supervision Bureau clearly require coal mining enterprises in China to use the water inrush coefficient method as the standard in water inrush prediction. Therefore, this formula is also used to calculate the no. 14 limestone aquifer water inrush coefficient of the floor of the 16104 working face in the Luxi coal mine.

The calculation formula is as follows:

$$T = P/M \tag{1}$$

T is the water inrush coefficient (MPa/m), P is the water pressure of the floor of aquiclude (MPa). M is the thickness of aquiclude (m).

Formula 1 is applicable to the coal working face. According to the actual data in China, the water inrush coefficient of the section with structural damage to the floor is generally not more than 0.06 MPa/m, and that of the section with complete aquiclude and no fracturing structural damage is not more than 0.1 MPa/m. The concept of the water inrush coefficient is clear, and its formula is simple and practical. Although there are only two simple factors—the water pressure P and the thickness of aquiclude M—in the expression, they reflect the comprehensive effect of water inrush factors. It has played a positive role in coal mine production, so it has been used thus far.

According to the water level observation data from different time periods during the fourth landing, the water inrush coefficient of the no. 14 limestone aquifer (Table 4) was calculated, and the contour map of the water inrush coefficient was drawn (Fig. 11).

According to the "detailed rules for prevention and control of water disasters in coal mines", the theoretical evaluation criteria for the water inrush coefficient are as follows:

Table 4 Water inrush coefficient table of the 16104 working face

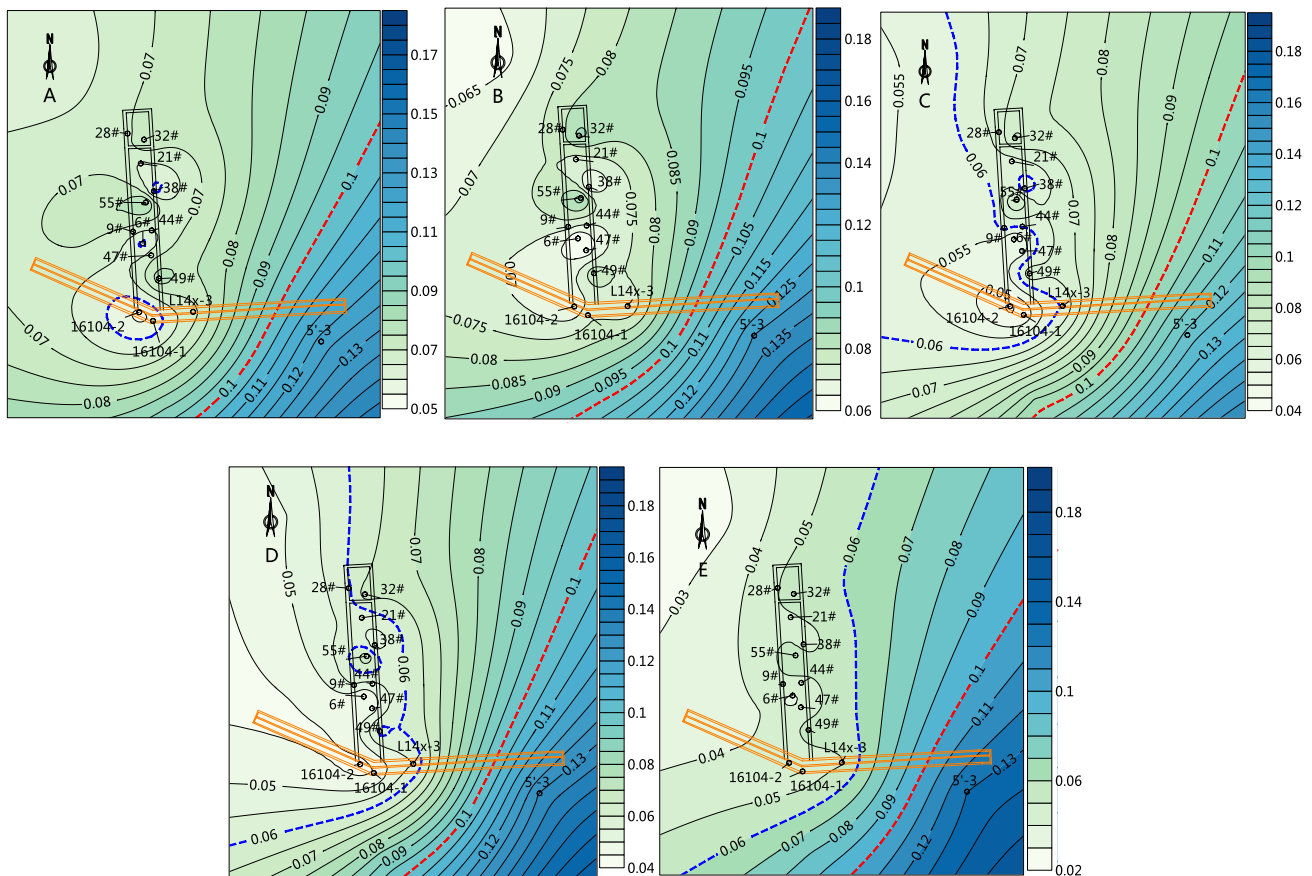| Hole number	Water inrush coefficient on August 14	Water inrush coefficient on September 3	Water inrush coefficient on September 3	Water inrush coefficient on September 17
6#	0.058	0.050	0.045	0.038
9#	0.067	0.062	0.055	0.047
21#	0.064	0.063	0.056	0.048
28#	0.068	0.067	0.059	0.049
32#	0.075	0.076	0.067	0.058
38#	0.058	0.056	0.051	0.044
44#	0.065	0.060	0.054	0.047
47#	0.068	0.053	0.047	0.041
49#	0.078	0.069	0.062	0.055
55#	0.082	0.078	0.069	0.060
L14x-3	0.068	0.060	0.055	0.049
16104-1	0.056	/	/	/
16104-2	0.054	/	/	/
5′-3	0.122	0.122	0.130	0.13

Fig. 11 Water inrush coefficient of the 16104 working face in the dewatering test

Block section with floor

damaged by structure : $T < 0.06\,\text{MPa/m}$ Safe area

$T \geq 0.06\,\text{MPa/m}$ Dangerous area

Block section with intact floor : $T < 0.1\,\text{MPa/m}$ Safe area

$T \geq 0.1\,\text{MPa/m}$ Dangerous area.

Considering the safe mining in 16104 working face, the drainage of no. 14 limestone aquifer is assessed by the minimum critical value of water inrush coefficient (0.06 MPa/m) of block section with floor damaged by structure. As can be noted from Fig. 11a, in the first stage, the maximum discharge rate of water occurs at the same time in the four boreholes of 16#, 24#, 37#, and 52#. In the stable stage, only the local water inrush coefficients near the boreholes of 6#, 38#, 16104-1 and 16104-2 are below 0.06 MPa/m, while the other regional water inrush coefficients are still above 0.06 MPa/m. Therefore, it is very difficult for the local discharge in the northern part of the working face to fall below the safe water level.

At the end of the third stage, the water level in the working face is in a state of recovery due to the reduced discharge

(Fig. 11b). Four days after the fourth stage began, the water inrush coefficient of the southern half of the 16104 face basically dropped below 0.06 MPa/m (Fig. 11c). After 6 days of drainage, the water inrush coefficient of the southern part of the working face basically dropped below 0.06 MPa/m, except that of hole 55# (Fig. 11d). After 14 days of drainage, the water inrush coefficients of the whole 16104 face and the surrounding area had dropped below 0.06 MPa/m (Fig. 11e).

It can be seen that the no. 14 limestone aquifer in the whole working face can be dredged at 240 m³/h. After approximately half a month, the water level can be lowered below the safe water level. The dredging effect is apparent. These results demonstrate that the no. 14 limestone aquifer has a good dredging ability. To ensure the safety of mining, the method of edge dredging and edge mining can be adopted on the basis of floor grouting in the subsequent mining period.

Discussion

During the dewatering test, the flow rate of the water discharge hole in the first stage dropped significantly, and the total water discharge gradually decreased from the maximum

of about 340 to 179 m^3/h. Affected by the water discharge of the group of holes in the working face, the actual flow rate of each water discharge hole has different degrees of attenuation than that during drilling verification, which shows that the no. 14 limestone aquifer in the study area is generally weak in water yield. At the same time, no. 14 limestone aquifer water level in each stage of the dewatering test showed the same change trend, and all experienced three stages: the initial instantaneous change stage, the rapid transition stage, and the long and stable stage. The instantaneous change of the water level reflects the good connectivity of the no. 14 limestone aquifer in the study area, and the long stable section indicates poor recharge. In short, the no. 14 limestone aquifer in the study area is generally characterized by weak water yield, good connectivity and poor supply conditions. The threat to mining No.16 coal seam can be relieved by drainage and pressure reduction.

This paper examines the observation data during the dewatering test. The water level change of the A2 observation hole is inconsistent with other Ordovician limestone aquifer observation holes. During the test, the water level of A2 hole dropped by 7.9 m and the characteristics of the water level curve were similar to those of no. 14 limestone aquifer water levels. Therefore, it is inferred that there is a connection channel between Ordovician and no. 14 limestone aquifers, which strengthen the hydraulic connection between the two aquifers in the area.

Conclusions

This paper presents a case study on the prevention and treatment of the thin limestone aquifers in the floor of the Luxi coal mine in Jining City, Shandong Province, China. Through hydrogeological exploration and drainage tests on the 16104 working face, the abnormal water yield area in the working face was proven, and the hydrogeological situation of the no. 14 limestone aquifer was determined through a drainage test. In the study area, the hydrogeology of the aquifer in the coal seam floor was ascertained, and the feasibility of drainage and depressurization of the aquifer in the coal seam floor was studied. This method can be theoretically more accurately verify the hydrogeological conditions of the aquifer in the coal floor and grasp the hydraulic connection of each aquifer.

Three geophysical exploration methods were carried out in the study area. The results show that there is abnormal water yield areas in the floor of the northern, central and southern parts of the working face. Then drilling verification is carried out for those areas detected by geophysical exploration, and the accuracy of geophysical exploration results is verified by the water inflow data of a single borehole. According to the results of geophysical exploration and

drilling, the stage of water release test is designed, the location of water release hole and observation hole is arranged in the test process, and the hydrogeological characteristics of the no. 14 limestone aquifer and its hydraulic connection with the Ordovician limestone aquifer are ascertained.

The water level observation data and water quality test data during the dewatering test were used to analyze the hydraulic connection between the no. 14 and Ordovician limestone aquifers in the working face. Observation data of the water level show that during the experiment, the change of the water level of the Ordovician limestone aquifer has a certain correlation with the discharge of the no. 14 limestone aquifer, indicating that there is a hydraulic connection between the two aquifers, but most of the observation holes of the Ordovician limestone aquifer have a small decrease in water level. It shows that the hydraulic connection between the two aquifers is weak. Hydrochemistry type of Ordovician limestone aquifer water is the same as that of the no. 14 limestone water, and the two aquifers have similar content of conventional ions. In addition, during the test, there was no significant change in the ion content of the no. 14 limestone aquifer groundwater before the test, so it was difficult to analyze the hydraulic connection between the Ordovician and no. 14 limestone aquifer in the working face by conventional hydrochemical methods.

In this paper, the feasibility of discharging in mining is studied. The results demonstrate that the no. 14 limestone aquifer can be dredged and lowered to below the safe water level within 15 days after a total depressurization rate of 240 m^3/h is implemented in the north, middle and south of the working face. The effect of drainage to a low water level is apparent and shows that the no. 14 limestone aquifer has a good ability to drain and depressurize. To ensure the safety of mining, on the basis of floor grouting, the method of sparse mining can be adopted during mining.

References

An XL (2018) Water prevention and control technology for coal seam floor grouting with high horizontal–vertical ratio ground oriented horizontal hole. Coal Sci Technol 46(11):126–132. https://doi.org/10.13199/j.cnki.cst.2018.11.020

Bu WK, Xu H (2011) Analysis on reverse fault activation and water inrush possibility for coal mining above confined aquifer in a mining area. J China Coal Soc 36(07):1177–1183. https://doi.org/10.13225/j.cnki.jccs.2011.07.018

Chen ZH, Hu ZP, Li H et al (2011) Fracture mechanical model and criteria of insidious fault water inrush in coal mines. J China

Univ Min Technol 40(05):673–677. https://doi.org/10.1007/s12583-011-0163-z

Chen SJ, Wang HL, Wang HY et al (2016a) Strip coal pillar design based on estimated surface subsidence in eastern China. Rock Mech Rock Eng 49(9):3829–3838. https://doi.org/10.1007/s00603-016-0988-y

Chen SJ, Yin DW, Cao FW, Liu Y, Ren K (2016b) An overview of integrated surface subsidence-reducing technology in mining areas of China. Nat Hazards 81:1129–1145. https://doi.org/10.1007/s11069-015-2123-x

Guo QG (2016) Research on China's coalmine safety regulatory capture: formation mechanism, double impact and governance effect. Ph.D. Thesis, Dongbei University of Finance and Economics **(in Chinese with English abstract)**

Guo WJ, Wang HL, Chen SJ (2016) Coal pillar safety and surface deformation characteristics of wide strip pillar mining in deep mine. Arab J Geosci 9(2):137. https://doi.org/10.1007/s12517-015-2233-5

Han WW, Li SC, Zhang QS et al (2013) A comprehensive analysis method for searching weak zones of grouting curtain in mines. Chin J Rock Mech Eng 32(03):512–519. https://doi.org/10.3969/j.issn.1000-6915.2013.03.010

Ji GZ, Wei JC, Yang ST et al (2018) Three-component polarization migration of channel waves for prediction ahead of coal roadway. J Appl Geophys 159:475–483. https://doi.org/10.1016/j.jappgeo.2018.09.028

Jiang T (2017) Analysis of water discharge test of III610 face in Yangzhuang coal mine. Papers collection of 2017 Academic Forum of Mine Geology Professional Committee of China Coal Association

Kuscer D (1991) Hydrological regime of the water inrush into the Kotredez Coal Mine (Slovenia, Yugoslavia). Mine Water Environ 10(1):93–101. https://doi.org/10.1007/BF02914811

LaMoreaux JW, Wu Q, Zhou WF (2014) New development in theory and practice in mine water control in China. Carbonate Evaporite 29(2):141–145. https://doi.org/10.1007/s13146-014-0204-7

Li BY (1999) "Down three zones" in the prediction of the water inrush from coalbed floor aquifer-theory, development and application. J Shandong Inst Min Technol (Nat Sci) 18(04):11–18

Li T, Gao Y, Chen W (2018a) Characteristics of deep Ordovician limestone water and its concentrated application in Ordovician limestone water disaster prevention. J China Coal Soc 43(S1):262–268. https://doi.org/10.13225/j.cnki.jccs.2017.3001

Li LY, Wei JC, Yin HY et al (2018b) Influence of sedimentary facies on reservoir quality and distribution of diagenetic features in the Funing Formation, Wanglongzhuang Oilfield, Subei Basin, Eastern China. Arab J Geosci 11(15):432–438. https://doi.org/10.1007/s12517-018-3745-6

Li YE, Ma NJ, Ma J et al (2018c) Surrounding rock's failure characteristic and rational location of floor gas drainage roadway above deep confined water. J China Coal Soc 43(09):2491–2500. https://doi.org/10.13225/j.cnki.jccs.2017.1768

Liu TQ (1995) Present situation and prospect of coal mining technology of under buildings, railways and water-bodies and above aquifer. Coal Sci Technol 23(1):5–7

Liu YJ, Xue JH, Yuan L et al (2017) Numerical test and mechanism analysis of water-inrush on soft rock floor. J China Coal Soc 42(12):3255–3261. https://doi.org/10.13225/j.cnki.jccs.2017.1107

Mironenko V, Strelsky F (1993) Hydrogeomechanical problems in mining. Mine Water Environ 12(1):35–40. https://doi.org/10.1007/BF02914797

Motyka J, Pulido-Bosch A (1985) Karstic phenomena in calcareous-dolomitic rocks and their influence over the inrushes of water in lead-zinc mines in Olkusz region (South of Poland). Int J Mine Water 4(2):1–11. https://doi.org/10.1007/BF02504832

Pan GY, Wang PL (2011) The feasibility study on Cambrian limestone water discharging based on large dewatering test of group holes.

J Henan Polytech Univ (Nat Sci) 30(06):674–678. https://doi.org/10.16186/j.cnki.1673-9787.2011.06.025

Qian MG, Liu XX, Li LJ (1995) Mechanism for the fracyure behaviours of main floor in longwall mining. Chin J Geotech Eng 17(6):56–61

Qiu M, Shi LQ, Teng C et al (2016) Assessment of water inrush risk using the fuzzy Delphi analytic hierarchy process and grey relational analysis in the Liangzhuang Coal Mine, China. Mine Water Environ 36(1):1–12. https://doi.org/10.1007/s10230-016-0391-7

Sammarco O, Eng D (1986) Spontaneous inrushes of water in underground mines. Int J Mine Water 5(3):29–41. https://doi.org/10.1007/BF02498099

Shi LQ, Han J (2015) Theory and practice of dividing coal mining area floor into four-zone. J China Univ Min Technol 34(1):16–23. https://doi.org/10.3321/j.issn:1000-1964.2005.01.004

Shi LQ, Singh RN (2001) Study of mine water inrush from floor strata through faults. Mine Water Environ 20(3):140–147. https://doi.org/10.1007/s10230-001-8095-y

Shi SQ, Wei JC, Xie DL et al (2019) Prediction analysis model for groundwater potential based on set pair analysis of a confined aquifer overlying a mining area. Arab J Geosci 12:115. https://doi.org/10.1007/s12517-019-4267-6

Song ZQ, Hao J, Tang JQ et al (2013) Study on water inrush from fault's prevention and control theory. J China Coal Soc 38(09):1511–1515. https://doi.org/10.13225/j.cnki.jccs.2013.09.011

Sun J, Wang LG (2013) Floor fault water-inrush prediction based on catastrophe analysis of micro-seismic signals. J China Coal Soc 38(08):1404–1410. https://doi.org/10.13225/j.cnki.jccs.2013.08.026

Sun WJ, Wu Q, Liu HL et al (2015) Prediction and assessment of the disturbances of the coal mining in Kailuan to karst groundwater system. Phys Chem Earth 89–90:136–144. https://doi.org/10.1016/j.pce.2015.10.008

Sun WJ, Zhou WF, Jiao J (2016) Hydrogeological classification and water inrush accidents in China's coal mines. Mine Water Environ 35:214–220. https://doi.org/10.1007/s10230-015-0363-3

Wang ZY (1992) Analysis and calculation of max depth of floor zero position failure zone. Coal Sci Technol 2(2–6):60–61

Wang H, Du JQ, Li JS (2010) Advance in tracer transfer regulation and research method of dewatering and tracing test in coalmine. Coal Geol Explor 38(05):28–33. https://doi.org/10.3969/j.issn.1001-1986.2010.05.006

Wei JC, Wu FZ, Yin HY, Guo JB, Xie DL, Xiao LL, Zhi HF, Liliana L (2017) Formation and height of the interconnected fractures zone after extraction of thick coal seams with weak overburden in western China. Mine Water Environ 36(1):59–66. https://doi.org/10.1007/s10230-016-0396-2

Wu Q (2014) Progress, problems and prospects of prevention and control technology of mine water and reutilization in China. J China Coal Soc 39(05):795–805. https://doi.org/10.13225/j.cnki.jccs.2014.0478

Wu Q, Xu H, Zhao YW, Du YZ, Zhang XY, Mu WP, Yao Y (2018) Cloud-based smart emergency rescue system and its application in mine water disaster. J China Coal Soc 43(10):2261–2267. https://doi.org/10.13225/j.cnki.jccs.2018.0899

Xu JL, Qian MG (2004) Study and application of mining-induced fracture distribution in green mining. J China Univ Min Technol 32(2):141–144. https://doi.org/10.3321/j.issn:1000-1964.2004.02.004

Xu YC, Li JH, Liu BZ (2014) Reinforcement of working face by grouting in floor in Jiaozuo coal mining area. Coal Geol Explor 42(04):50–54. https://doi.org/10.3969/j.issn.1001-1986.2014.04.011

Xu DJ, Peng SP, Xiang SY et al (2015) The effects of caving of a coal mine's immediate roof on floor strata failure and water inrush.

Mine Water Environ 35(3):1–13. https://doi.org/10.1007/s10230-015-0368-y

Xu YC, Xie XF, Liu SQ et al (2017) Quantitative determination of mechanical property of "enhance-damage" for floor rock mass in grouting reinforcement working face. J Min Saf Eng 34(06):1186–1193. https://doi.org/10.13545/j.cnki.jmse.2017.06.023

Yang SM, Li SY (2015) Main water disaster and its countermeasures in Yima mining area. Saf Coal Mines 42(03):106–109. https://doi.org/10.13347/j.cnki.mkaq.2015.02.048

Yang XH, Wang YH, Cai XJ et al (2016) Study on hidden hazard factors and the prevention measures in Linxi Mine of Kiluan mining area. Coal Eng 48(12):59–62. https://doi.org/10.11799/ce201612019

Yin HY, Shi YL, Niu HG et al (2017) A GIS-based model of potential groundwater yield zonation for a sandstone aquifer in the Juye Coalfield, Shangdong, China. J Hydrol 557:434–447. https://doi.org/10.1016/j.jhydrol.2017.12.043

Yin HY, Zhou WF, LaMoreaux JW (2018) Water inrush conceptual site models for coal mines of China. Environ Earth Sci 77:746. https://doi.org/10.1007/s12665-018-7920-6

Yin HY, Sang SZ, Xie DL et al (2019) A numerical simulation technique to study fault activation characteristics during mining between fault bundles. Environ Earth Sci. https://doi.org/10.1007/s12665-019-8142-2

Yu XG, Han J, Shi LQ et al (2017) Application of a BP neural network in predicting destroyed floor depth caused by underground pressure. Environ Earth Sci 76(15):535. https://doi.org/10.1007/s12665-017-6878-0

Zhai XR, Wu WJ, Han DY (2014) Aquifer parameter calculation of pumping test of group holes with recharge boundary. J China Univ Min Technol 43(05):837–840 + 863. https://doi.org/10.13247/j.cnki.jcumt.000089

Zhang JG, Song DX (2013) Technology of coal limestone water regional control in Pingdingshan mining area. Coal Sci Technol 41(9):71–74. https://doi.org/10.13199/j.cnki.cst.2013.09.017

Zhang JF, Zhang HL, Meng D et al (2009) Numerical simulation of rock deformation and seepage field with a full-water karstic collapse column under mining influence. Chin J Rock Mech Eng 28(S1):2824–2829

Zhao SQ, Wu Q, Yin SX (2016) Scientific and quick rescue for water hazards of coal mines. Coal Eng 48(S2):9–11. https://doi.org/10.11799/ce201611045